A macrocyclic ‘Co^0’ complex: the relevance of ligand non-innocence to reactivity†

Manuel Kaspar,[a] Philipp J. Altmann,[a] Alexander Pöthig,[a] Stephen Sproules,[b] Corinna R. Hess*[a]

[a] Department of Chemistry and Catalysis Research Center, Technische Universität München, Lichtenbergstrasse 4, D-85747, Garching (Germany). Email: corinna.hess@ch.tum.de

[b] WestCHEM, School of Chemistry, University of Glasgow, Glasgow G12 8QQ (UK)

†Electronic Supplementary Information (ESI) available: Experimental details for the synthesis of **1** and **3**, spectroscopic data and CIFs. See DOI: 10.1039/x0xx00000x

We present a formally zero-valent compound, [Co(Mabiq)Na(OEt$_2$)]$_2$ (1). The complex was characterized by crystallographic, spectroscopic and DFT computational methods. The electronic structure is described as a Co^{II}–(ligand-biradical). Compound 1 is reactive toward proton sources; Co^{I} or Co^{II} products result, depending on the source of protons used. The redox non-innocence of the Mabiq ligand, which accepts both protons and electrons, has important ramifications for reactivity.

The advancement of solar fuel technologies is vital for the global progression toward renewable energy sources.[1] The development of robust and inexpensive catalysts for the conversion of protons or CO_2 into energy-rich chemicals is integral to these efforts.[2-4] Among the suitable noble-metal free complexes, molecular cobalt compounds have demonstrated significant promise as both electro- and photocatalysts for both reactions.[5-8] These compounds encompass a diverse array based on unsaturated N_4-macrocyclic, pyridyldiimine, polypyridine, triphos and dithiolene ligands.[9-17] The reactivity of the complexes hinges on the formation of low-valent forms: typically a Co^{I} species is invoked in catalytic cycles for H_2 evolution.[6,7] However, in several cases, generation of the more nucleophilic Co^{0} species is required for reactivity of the complexes.[6,7,9,15,17-19] A few Co^{I} compounds have been isolated among known catalysts.[9,14,20] However, the Co^{0} species remains elusive among these systems, its properties gleaned only on the basis of indirect and theoretical evidence.[21,22] The electronic structure of the zero-valent intermediate is of further intrigue, as this reduced form might in actuality possess substantial ligand radical character. A true Co^{0} compound may well be supported by triphos and macrocyclic aminopyridine ligands.[9,14] However, the alternative Co^{I}L$^{\bullet}$ description is recognized as a more accurate depiction of the doubly-reduced species among compounds containing porphyrin and diimine-based ligands, for example.[6,18,19,23] This ligand non-innocence may have important consequences for proton coupled electron transfer processes associated with both H_2 evolution and CO_2 activation.[12,18,19,23-25] The Co^{0} complex is, therefore, a missing yet pivotal piece of mechanistic puzzles. Furthermore, the

reactivity of this supernucleophile remains unexplored. Insight into the electronic structure of the doubly reduced species will guide our understanding of its chemistry.

Toward this end, we have now isolated a doubly reduced, *formally* zero-valent compound, $[Co(Mabiq)Na(OEt_2)]_2$ (**1**, Scheme 1), based on our N_4-macrocyclic Mabiq ligand. Compound **1** completes the electron transfer series of our Co-Mabiq complexes, which already included the formally monovalent Co(Mabiq) (**2**),[26] and now encompasses the full complement of formal oxidation states ($0 \rightarrow +3$) invoked in the catalytic cycles of the HER and CO_2 reduction. The characterization of **1** by crystallographic, spectroscopic and DFT computational methods is described herein. Preliminary studies examining the reactivity of **1** toward proton source also are presented. The results already highlight ramifications of proton and electron storage by the redox-active Mabiq ligand for reactivity.

In association with the present work, a new form of the cobaltous-Mabiq complex, $[Co(Mabiq)(THF)](PF_6)$ (**3**), also was synthesized. The molecular structure (Figure S1) resembles that of the previously isolated Co(Mabiq)Cl,[26] except a solvent molecule occupies the axial position in lieu of the chloride ligand. Compound **3** was deemed more suitable for comparison of products obtained in the reaction of **1**. The electronic spectrum of **3** closely resembles that of Co(Mabiq)Cl, with minor shifts in the absorption bands. The EPR spectrum recorded at room temperature is consistent with a low-spin Co^{II} center (Figure 1). The 8-line pattern from coupling with the ^{59}Co $I = {}^7/_2$ (100%) isotope is larger than for [Co(Mabiq)Cl].[26]

The title Co^0 compound was obtained upon treatment of Co(Mabiq) with one equivalent of Na in THF, yielding the dark red **1**. The compound is dimeric in the solid state (Figure 2); the two bipyrimidine (bpm) units are within π-stacking distance (3.47 Å). A sodium ion coordinates the external diimine group of each monomeric unit, and further promotes association of the two macrocycles. The short contacts between the alkali metal situated in the bpm moiety of one

molecule, and the N-atom of the neighboring bpm (Na–N1a = 2.676(3) Å) betrays significant electron density on the biquinazolines.[27] The shortened C–C and longer C–N bond distances of the bpm diimine moiety, in comparison to those of **2** and **3** (Table S2), allude to ligand-centered reduction.

The electronic spectrum of **1** (Figure S5) shares several features with that of **2**, notably intense bands centered at 525 nm, along with NIR absorptions, none of which appear in the spectrum of the cobaltous **3**. However, compound **1** exhibits a unique, pronounced transition at 442 nm, as well as shoulders (ca. 600 and 650 nm) to the 532 nm absorption. A transition at 429 nm also features in the spectrum of **3**, which otherwise is distinguished by a series of bands in the visible region (550 – 700 nm). Compound **1** most likely exists as a monomer in solution; the π- and intermolecular Na-N interactions that govern association of the macrocycles in the solid state are unlikely to persist in solvent. The EPR spectrum of **1** is diagnostic of a ligand-centered unpaired spin with a featureless line, with g_{iso} = 2.0029 (Figures 1 and S25). A satisfactory fit included a miniscule $A\{^{59}Co\}$ coupling of 1.05×10^{-4} cm^{-1} commensurate with the <0.5% Co content of the SOMO (*vide infra*). The addition of 15-Crown-5 to a solution of **1** had no effect on the EPR spectrum.

The electronic structure of **2** was previously described by $Co^{I}(Mabiq^{-}) \leftrightarrow Co^{II}(Mabiq^{2-\bullet})$ resonance forms on the basis of density functional (DFT) calculations.[26] $[Co^{I}(Mabiq^{2-\bullet})]^{-}$ and $[Co^{II}(Mabiq^{3-})]^{-}$, containing the one- or two-electron reduced macrocycle, likewise offer alternate formulations of the formally zero-valent complex. DFT (B3LYP) calculations on the monomeric form of the compound, $[Co(Mabiq)Na(OEt_2)]$, yielded an open-shell solution supporting the $[Co^{II}(Mabiq^{3-})]^{-}$ description of **1**. The DFT-derived spin-density map (Figure 3) depicts two electrons of alpha-spin on the macrocycle, and one electron of beta-spin on the metal ion. Three doubly occupied metal-based orbitals can be identified by inspection of the

DFT-derived molecular orbitals (Figure S4) and the Loewdin population analysis. The unpaired electron on the cobalt ion resides in the *xz* orbital. The corresponding ligand-centered radical of opposite spin occupies a diketiminate π* orbital, as seen in the neutral series of compounds: $Co^{II}(Mabiq^{2-\bullet})$, $Fe^{II}(Mabiq^{2-\bullet})$ and $Zn^{II}(Mabiq^{2-\bullet})$.[26,28] However, the final SOMO in the MO depiction of **1** represents a bpm-based π* orbital. Although the first ligand-centered reduction consistently involves the diketiminate, the bpm clearly also is redox-active. The DFT results, denoting antiferromagnetic coupling between an $S = {}^1/_2$ Co^{II} ion and an $S = 1$ Mabiq di-radical, are consistent with the EPR data.

Compound **1** is indeed reactive toward proton sources (product spectra, Figure S6). A solution of **1** in THF immediately changes color from red to purple, upon addition of benzoic acid (5 equiv.). The product absorption spectrum indicates the formation of a Co^{I} species. The reaction of **1** with one equiv. *p*CA also produces a Co^{I} species; the product spectrum is again similar, but not identical, to that of **2**. At higher acid concentrations, further conversion to a Co^{II}-containing compound occurs. The product spectrum typifies a Co^{II} species, with the characteristic absorption features in the visible region, but does not precisely match that of **3**. For comparison, the addition of *p*CA to a solution of **2** likewise yields a Co^{II} compound; in this case, the product spectrum is superimposable with that of **3** (Figure S6), suggesting clean conversion to the oxidized form. The monovalent compound does not react with benzoic acid; as expected, the doubly-reduced **1** is more nucleophilic than **2**, such that it reacts even with weak acids.The products of the **1**/acid reaction mixtures were further analyzed by ^{1}H NMR spectroscopy (Figure S7 – S15). Two diamagnetic products are produced in the **1**/benzoic acid and **1**/*p*CA reactions (5 equiv. benzoic acid; 1 equiv. *p*CA), which could be separated by chromatography. The primary reaction product corresponds to **2**, as evidenced by the NMR spectrum (Figure 4, bottom). The NMR spectrum of the second product (30 – 50%) exhibits eleven proton

resonances in the aromatic region, denoting desymmetrization of the macrocyclic ligand (Figure 4, top). Three singlets are present at 7.47, 7.30 and 6.52 ppm. The resonance at 7.30 ppm can be assigned to the diketiminate proton. The additional two signals at 6.52 and 7.47 ppm correspond to protons situated at bpm N and C atoms, respectively, based on the COSY, HSQC and HMBC spectra (Figure S13 – S15).

The one-electron oxidized, diamagnetic [Co(MabiqH$_2$)] (**[2-H$_2$]**), containing a doubly protonated Mabiq ligand describes the second product in the reaction of **1** with acid. The molecular structure of **[2-H$_2$]** (Figure S29) offers further evidence that the bpm unit is altered. The negatively charged diimine component of **1** readily takes up the acidic protons. No evidence of H_2 was observed by NMR for any of the **1**/acid reactions. We thus propose that the formation of **[2-H$_2$]** could proceed according to Scheme 2.

The initial protonation of **1** leads to the formation of a [Co^{II}(MabiqH$_2$)]$^-$ species. Subsequent intermolecular electron transfer involving a second molecule of **1** yields a mixture of **2** and **[2-H$_2$]**, as observed by NMR.

We note that ligand protonation does not generally ensue under acidic conditions. Mass spectrometry data (Figures S16 – S23) of **3**/acid mixtures shows only a peak of *m/*z = 600 ([M]$^+$), corresponding to the parent complex. Ligand protonation also does not occur upon addition of benzoic acid to a solution of **2**, whereas with *p*CA, an additional peak of *m/z* = 602 ([M+2]$^+$) is observed, as for the **1**/acid reactions. Radical character in **2** may likewise render the macrocycle susceptible to modification by strong acids.

The reactivity of **1** parallels the behavior predicted in computational studies for low-valent porphyrin compounds. The generation of a phlorin intermediate in the mechanism of H_2 evolution by 'Co^0'-porphyrins is thermodynamically favored over metal-hydride formation.[23] The preferred ligand protonation is a consequence of porphyrin radical character in the zero-

valent form. Doubly protonated porphyrin intermediates are generated in the HER by hangman porphyrins and require further reduction to effect H_2 release.[23,29]

Compound **[2-H$_2$]** does not appear to release H_2. No change was observed in the NMR spectrum of **[2-H$_2$]**, even upon heating of a sample to 50 °C. **[2-H$_2$]** also does not react appreciably with proton sources. Only minor changes in the absorption spectrum are observed upon addition of *p*CA (up to 15 equiv., THF; Figure S30). **[2-H$_2$]** also does not react with TEMPO-H.

Interestingly, the CV of **[2-H$_2$]** shows that the values for the $Co^{III/II}$ and $Co^{II/I}$ redox potentials are similar to those of **3** (Figure S31). Protonation of the bpm moiety appears to have a negligible influence on the metal center. Furthermore, the formal $Co^{II/I}$ couple may involve reduction of the diketiminate unit, as observed for **3**. This group is situated furthest away from the ligand protonation site. The $Co^{I/0}$ couple of the modified Mabiq complex exhibits the largest shift, by -100 mV, consistent with reduction of the bpm unit upon addition of the second electron. The electronic structure of **[2-H$_2$]** is analogous to that of **2**: the DFT-derived (B3LYP, BS1,1) spin density plot (Figure S32) again depicts the radical character of the ligand, with electron density localized on the diketiminate moiety. The differing reactivity of **2** and **[2-H$_2$]** toward proton sources is thus surprising. The reactivity of these one-electron reduced forms remains to be examined in detail.

The current work, focusing on the properties and reactivity of the formally zero-valent **1**, highlights important lessons for the use of redox active ligands in proton coupled electron transfer processes. The generation of zero-valent compounds is thought to be necessary for the reduction of weak acids by numerous HER catalysts. Since reduction of our cobaltous compound is clearly ligand-centered, the macrocycle rather than the metal takes up added protons. Consequently, our doubly reduced Co^{II}–(ligand-biradical) complex appears to be

unviable for the hydrogen evolution reaction. The 'zero-valent' and $M^{I}L^{\bullet}$ intermediates cited among other molecular systems should be examined in greater detail. A genuine Co^{0} intermediate likely will react with protons in a different manner to our complex, via a metal-hydride species that could effectively release H_2. However, among the many cobalt systems containing redox-active ligands, the ligand may likewise compete with the metal center for both electrons and protons. A greater understanding of the scenarios under which such ligand frameworks inhibit or support reactivity will be important for HER catalyst design. Regardless, the incorporation of non-innocent ligands in coordination complexes offers a powerful tool for other redox reactions,[30] and may in fact favor CO_2 redution.[19] The broader reactivity of the doubly-reduced **1** toward other substrates, including CO_2, will be explored in future work.

The authors thank Prof. Klaus Köhler for the use of his EPR spectrometer, and Dr. Carmen Haeßner for technical assistance. MK and PA thank the TUM Graduate School for financial support.

Notes and References

1. N. S. Lewis and D. G. Nocera, *Proc. Natl. Acad. Sci*, 2006, **103**, 15729-15735.
2. J. R. McKone, N. S. Lewis and H. B. Gray, *Chem. Mater.*, 2014, **26**, 407-414.
3. S. Berardi, S. Drouet, L. Francàs, C. Gimbert-Suriñach, M. Guttentag, C. Richmond, T. Stoll and A. Llobet, *Chem. Soc. Rev.*, 2014, **43**, 7501-7519.
4. M. Rakowski DuBois and D. L. DuBois, *Acc. Chem. Res.*, 2009, **42**, 1974-1982.
5. N. Kaeffer, M. Chavarot-Kerlidou and V. Artero, *Acc. Chem. Res.*, 2015, **48**, 1286-1295.
6. N. Queyriaux, R. T. Jane, J. Massin, V. Artero and M. Chavarot-Kerlidou, *Coord. Chem. Rev.*, 2015, **304-305**, 3-19.

7. J. R. McKone, S. C. Marinescu, B. S. Brunschwig, J. R. Winkler and H. B. Gray, *Chem. Sci.*, 2014, **5**, 865-878.

8. J. Bonin, A. Maurin and M. Robert, *Coord. Chem. Rev.*, 2017, **334**, 184-198.

9. S. C. Marinescu, J. R. Winkler and H. B. Gray, *Proc. Natl. Acad. Sci. U.S.A.*, 2012, **109**, 15127-15131.

10. V. Artero and M. Fontecave, *Chem. Soc. Rev.*, 2013, **42**, 2338-2356.

11. C. Costentin, H. Dridi and J.-M. Savéant, *J. Am. Chem. Soc.*, 2014, **136**, 13727-13734.

12. B. H. Solis and S. Hammes-Schiffer, *Inorg. Chem.*, 2014, **53**, 6427-6443.

13. J. L. Dempsey, J. R. Winkler and H. B. Gray, *J. Am. Chem. Soc.*, 2010, **132**, 1060-1065.

14. A. Chapovetsky, T. H. Do, R. Haiges, M. K. Takase and S. C. Marinescu, *J. Am. Chem. Soc.*, 2016, **138**, 5765-5768.

15. Z. Guo, S. Cheng, C. Cometto, E. Anxolabéhère-Mallart, S.-M.-. Ng, C.-C. Ko, G. Liu, L. Chen, M. Robert and T.-C.-. Lau, *J. Am. Chem. Soc.*, 2016, **138**, 9413-9416.

16. W. R. McNamara, Z. Han, P. J. Alperin, W. J. Brennessel, P. L. Holland and R. Eisenberg, *J. Am. Chem. Soc.*, 2011, **133**, 15368-15371.

17. C. H. Lee, D. K. Dogutan and D. G. Nocera, *J. Am. Chem. Soc.*, 2011, **133**, 8775-8777.

18. L. Tong, A. Kopecky, R. Zong, K. J. Gagnon, M. S. G. Ahlquist and R. P. Thummel, *Inorg. Chem.*, 2015, **54**, 7873-7884.

19. D. C. Lacy, C. C. L. McCrory and J. C. Peters, *Inorg. Chem.*, 2014, **53**, 4980-4988.

20. X. Hu, B. S. Brunschwig and J. C. Peters, *J. Am. Chem. Soc.*, 2007, **129**, 8988.

21. S. Ciurli, S. Gambarotta, C. Floriani, A. Chiesi- Villa and C. Guastini, *Angew. Chem. Int. Ed.*, 1986, **25**, 553-554.

22. A search of the CCDC (July 2016) revealed only a Co(0)-tetraphenylporphyrin (TPP) structure (see Ref. 17). The reactivity of the complex was not examined.

23. B. H. Solis, A. G. Maher, T. Honda, D. C. Powers, D. G. Nocera and S. Hammes-Schiffer, *ACS Catal.*, 2014, **4**, 4516-4526.

24. L. M. A. Quintana, S. I. Johnson, S. L. Corona, W. Villatoro, W. A. Goddard, M. K. Takase, D. G. VanderVelde, J. R. Winkler, H. B. Gray and J. D. Blakemore, *Proc. Natl. Acad. Sci. U.S.A.*, 2016, **113**, 6409-6414.

25. R. M. Bullock and M. L. Helm, *Acc. Chem. Res.*, 2015, **48**, 2017-2026.

26. E. V. Puttock, P. Banerjee, M. Kaspar, L. Drennan, D. S. Yufit, E. Bill, S. Sproules and C. R. Hess, *Inorg. Chem.*, 2015, **54**, 5864-5873.

27. $[Na(THF)_3]^+$ ions were also present in the molecular structure of the Co^0-TPP complex (Ref. 17), situated above and below the porphyrin; the reported Na-N(TPP) bond distances (2.766(5); 2.757(5) Å) are longer than the analogous Na-N(2a) bond distances of **1**.

28. P. Banerjee, A. Company, T. Weyhermüller, E. Bill and C. R. Hess, *Inorg. Chem.*, 2009, **48**, 2944-2955.

29. B. H. Solis, A. G. Maher, D. K. Dogutan, D. G. Nocera and S. Hammes-Schiffer, *Proc. Natl. Acad. Sci. U.S.A.*, 2016, DOI: 10.1073/pnas.1521834112, 485-492.

30. P. J. Chirik and K. Wieghardt, *Science*, 2010, **327**, 794.

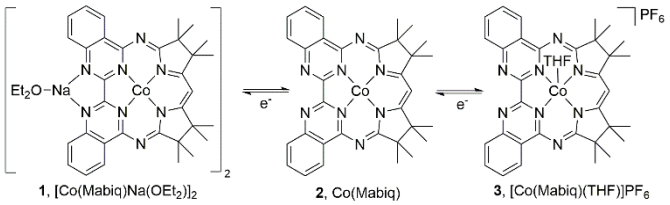

Scheme 1 Electron transfer series of Co-Mabiq compounds with formal metal valencies of 0 → +2

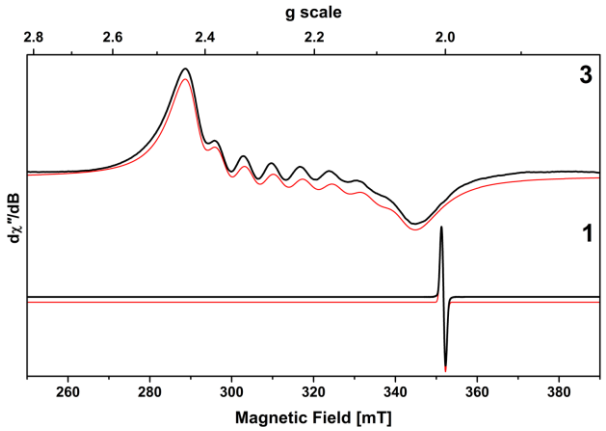

Fig. 1 X-band EPR spectra of **3** (CH_2Cl_2/toluene) and **1** (THF) Experimental data are represented by the black line and simulation by the red trace: **3**, g_{iso} = 2.224; A_{iso} = 74.2 × 10^{-4} cm^{-1}; **1**, g_{iso} = 2.0029; A_{iso} = 1.05 × 10^{-4} cm^{-1}.

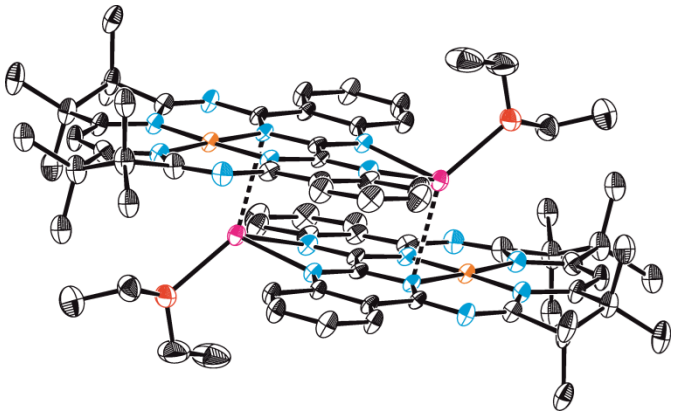

Fig. 2 Molecular structure of **1** (50% probability ellipsoids). Hydrogen atoms omitted for clarity.

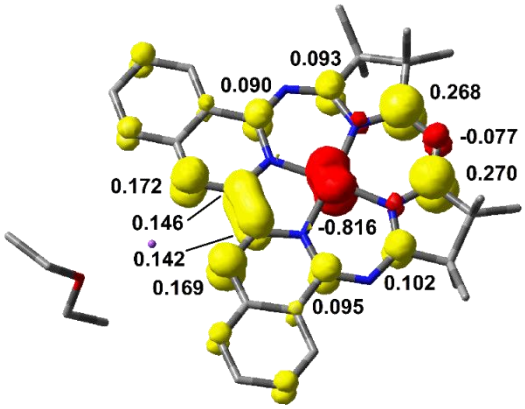

Fig. 3 DFT-derived (B3LYP) spin-density plot for the monomeric unit of **1** based on Löwdin population analysis.

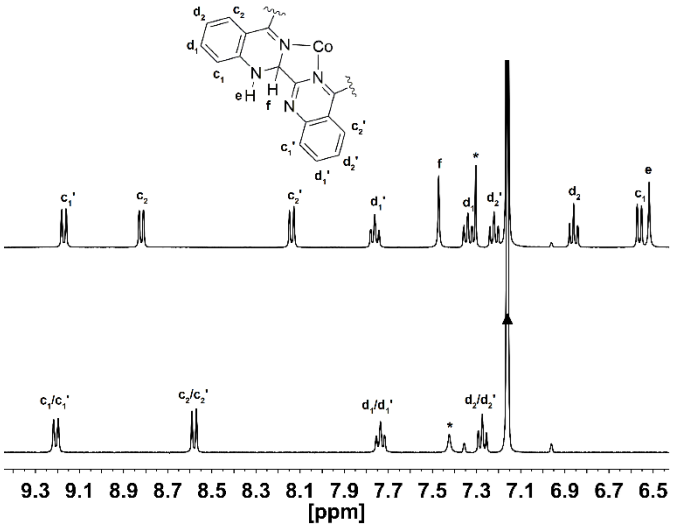

Fig. 4 ^{1}H NMR spectra (aromatic region; benzene-d_6 (▲)) of the two products of the **1**/benzoic reaction mixture: **2** (bottom) and (**[2-H₂]** (top). The diketiminate proton is denoted by the asterisk (*).

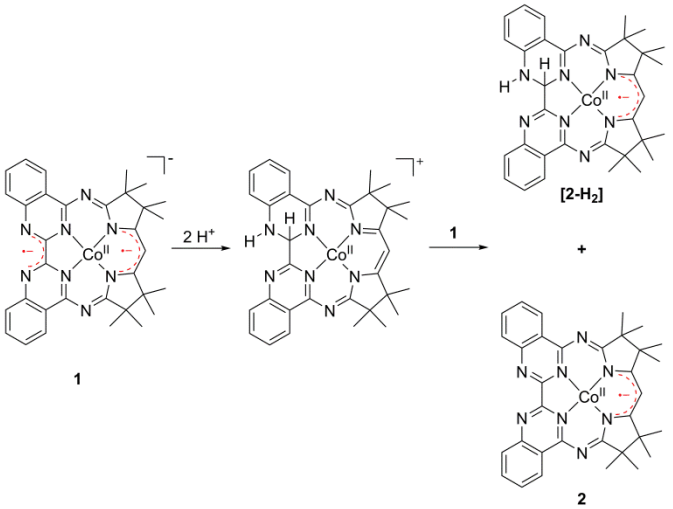

Scheme 2 Proposed reaction of **1** with acid to form **[2-H₂]**